*Tellus* (1982), *34*, 255–265

# Bifurcation properties of quasi-geostrophic, barotropic models and their relation to atmospheric blocking

By E. KÄLLEN*, *European Centre for Medium Range Weather Forecasts, Shinfield Park, Reading, Berkshire, RG2 9AX, England*

(Manuscript received July 13; in final form October 12, 1981)

ABSTRACT

The bifurcation properties of a low-order, barotropic model on the sphere with orographic and a Newtonian type of vorticity forcing are reviewed. The low-order model results that multiple equilibria develop as a result of a sufficiently strong, long-wave, orographic forcing and that a suitably positioned wave vorticity forcing can enhance this bifurcation mechanism are verified with a high resolution, spectral model. The high-resolution model is integrated in time to find stable steady states. Bifurcations into multiple equilibria appear as sudden jumps in the amplitudes of the model components when the forcing is slowly changing in time.

A limited diagnostic study of some blocking events in the Northern Hemisphere during the months January–March 1979 is also presented. Calculations of the mountain torque and the eddy activity in certain regions partly support the blocking mechanism originally proposed by Charney and DeVore, and further developed by Källén.

## 1. Introduction

Recently several authors have dealt with the non-linear properties of barotropic models to describe long waves in the atmosphere (Charney and DeVore, 1979; Wiin-Nielsen, 1979; Vickroy and Dutton, 1979; Davey, 1980, 1981; Källén, 1981). Low-order spectral representations of the non-linear barotropic vorticity equation have been analyzed and the bifurcation properties of these low-order systems have suggested a possible explanation for the atmospheric blocking phenomenon.

Charney and DeVore (1979) analyzed a beta plane model with orographic forcing in one wave component and momentum forcing in one zonal component. For sufficiently high values of the forcing parameters multiple equilibria developed and one of the stable equilibria could be interpreted as representing atmospheric blocking. Other stable equilibria which are possible with the same forcing parameters, have properties which are markedly different from the blocked stable equilibrium. Davey (1980, 1981) demonstrated that the same bifurcation mechanism exists in a beta-plane high resolution model as well as in a model of a rotating annulus. Källén (1981), hereafter called K81, showed that this bifurcation mechanism is also possible on a spherical geometry. Furthermore, it was demonstrated by K81 that a suitably positioned vorticity forcing in the same wave-component as the orography enhances the bifurcation mechanism obtained in the purely orographically forced case. Wiin-Nielsen (1979), using a low-order barotropic system on the sphere, demonstrated that vorticity forcing without orographic forcing may also give rise to a bifurcation. Comparisons with this study are, however, difficult due to a different selection of components.

This study will deal with a verification, using a high-resolution numerical model, of some of the low-order results found by K81. A spectral model, originally developed at the University of Reading, England, is integrated in time with the same simplified forcing as used in the low-order model. By varying some of the forcing components slowly

* On leave from: Department of Meterology, University of Stockholm, Arrhenius Laboratory, S-106 91 Stockholm, Sweden.



0040-2826/82/030255-11$02.50/0 

in time, sudden jumps from what appears to be quasi-stable states of the model are found. These jumps indicate the existence of multiple equilibria within certain regions of the model parameter space.

Additionally, some results from diagnostic studies of the mountain torque for the months January–February 1979 using FGGE-data will be presented. During this time period several blocking events occurred in the Northern Hemisphere, both in the Pacific and Atlantic areas. Calculations of the mountain torque and the eddy activity over certain regions will be presented. The results of these calculations suggest a possible coupling between the generation of a block in the atmospheric flow, the mountain torque and the eddy activity upstream of the blocking region. This coupling gives some support for the bifurcation mechanism presented in Sections 2 and 3, in explaining certain features of atmospheric blocking.

Section 2 will give a short review of the low-order model of K81 and a summary of the most important results. In Section 3 a comparison between the low-order model results and results from integrations with a high-resolution model will be made. Section 4 will deal with the diagnostic study.

## 2. Low-order model

The bifurcation properties of a low-order, spectral representation of the quasi-geostrophic, barotropic vorticity equation with orographic and momentum forcing will be analyzed in this section following K81. The governing equation in a non-dimensional form reads

$$\frac{\partial \zeta}{\partial t} = J(\zeta + h, \psi) - 2\frac{\partial \psi}{\partial \lambda} + \varepsilon(\zeta_E - \zeta) \tag{1}$$

where $\zeta$ is the vorticity, $\psi$ is the streamfunction, $t$ is time, $\zeta_E$ is the vorticity (or momentum) forcing, $J$ is the Jacobian with respect to $\lambda$ (longitude) and $\mu = \sin\varphi$, $\varphi$ is latitude, and $\varepsilon$ is the dissipation rate. The parameter representing the orography, $h$, can be related to a dimensional mountain height, $m$, via

$$h = 2\mu_0 A(p_0)\frac{m}{H} \tag{2}$$

where $H$ is the scale height of the barotropic model and $2\mu_0 A(p_0)$ is approximately equal to one. This parameter depends on the assumption of an equivalent barotropic atmosphere. For details of the derivation of eqs. (1) and (2), see K81.

A low-order representation of eq. (1) is found through an expansion of the space dependent variables in a series of spherical harmonics. The expansion is truncated at a very low order, just leaving a few terms in the series to describe the flow pattern. The main advantage of a low-order system is that it can be handled analytically and the properties of the low-order model may be used as a guide when performing numerical experiments with a high-resolution model.

The space-dependent variables to be expanded are the vorticity, the vorticity forcing and the orography. The expansion in spherical harmonics may be written

$$\begin{pmatrix} \zeta \\ \zeta_E \\ h \end{pmatrix} = \sum_{k,n} \begin{pmatrix} \zeta_{k,n} \\ \zeta_{E_{k,n}} \\ h_{k,n} \end{pmatrix} P_n^k(\mu)\, e^{ik\lambda} \tag{3}$$

where $P_n^k(\mu)$ is an associated Legendre polynomial of order $n$ and zonal wave number $k$, normalized according to

$$\tfrac{1}{2}\int_{-1}^{1} [P_n^k(\mu)]^2\, d\mu = 1 \tag{4}$$

Through the definition $\zeta = \nabla^2 \psi$ we have, for each component,

$$\zeta_{k,n} = -c_n \psi_{k,n} \tag{5}$$

where $c_n = n(n+1)$.

Inserting the expansion (3) into the barotropic vorticity equation (1) and making use of the orthogonality properties of the spherical harmonics, we obtain a set of ordinary differential equations governing the time evolution of the individual spectral components. The components retained in the low-order model are chosen in such a way that the non-linearity present in the $J(\zeta + h, \psi)$ term of eq. (1) is taken into account to as large an extent as possible. The details of how the optimal choice of components can be made is given in K81. The resulting low-order stream function expansion is

$$\begin{aligned} \psi(\mu, \lambda, t) = {} & -u_0(t)\, P_1(\mu) + z(t)\, P_n(\mu) \\ & + (x_1(t)\cos l\lambda + y_1(t)\sin l\lambda)\, P_{n_1}^l(\mu) \\ & + (x_2(t)\cos l\lambda + y_2(t)\sin l\lambda)\, P_{n_2}^l(\mu) \end{aligned} \tag{6}$$

Two purely zonal components, with amplitudes $u_0$ and $z$, and four wave components with amplitudes $x_1$, $y_1$, $x_2$ and $y_2$ with the same zonal wavenumber $l$ but different orders of the Legendre polynomials, $n_1$ and $n_2$, are included. The vorticity forcing is assumed to be present in the zonal component which describes a solid body rotation of the whole barotropic atmosphere ($u_0$), and in two of the wave components ($x_1$ and $y_1$) with amplitudes $u_{0E}$, $x_{1E}$ and $y_{1E}$ respectively. Orography is included in only one of the wave components $(l, n_1)$ with an amplitude $h_1$. The six equations describing the time evolution of the spectral coefficients are

$$\begin{aligned}
\dot{u}_0 &= h_1 \delta_1 y_1 + \varepsilon(u_{0E} - u_0)\\
\dot{z} &= \gamma_1(x_2 y_1 - x_1 y_2) - h_1(\delta_2 y_2 + \delta_3 y_1) - \varepsilon z\\
\dot{x}_1 &= z(\gamma_2 y_2 + \gamma_4 y_1) + y_1(\beta_1 - \alpha_1 u_o) + \varepsilon(x_{1E} - x_1)\\
\dot{y}_1 &= -z(\gamma_2 x_2 + \gamma_4 x_1) - x_1(\beta_1 - \alpha_1 u_0) + h_1(\delta_5 z - \delta_4 u_0) + \varepsilon(y_{1E} - y_1)\\
\dot{x}_2 &= z(\gamma_3 y_1 + \gamma_5 y_2) + y_2(\beta_2 - \alpha_2 u_0) - \varepsilon x_2\\
\dot{y}_2 &= -z(\gamma_3 x_1 + \gamma_5 x_2) - x_2(\beta_2 - \alpha_2 u_0) + h_1 \delta_6 z - \varepsilon y_2
\end{aligned} \tag{7}$$

where

$$\alpha_1 = \sqrt{3}\, l(1 - 2c_1^{-1}), \quad \alpha_2 = \sqrt{3}\, l(1 - 2c_2^{-1}),$$

$$\beta_1 = \frac{2l}{c_1}, \quad \beta_2 = \frac{2l}{c_2}, \quad \gamma_1 = \frac{Il}{4c}(c_2 - c_1),$$

$$\gamma_2 = \frac{Il}{2c_1}(c_2 - c), \quad \gamma_3 = \frac{Il}{2c_2}(c_1 - c),$$

$$\gamma_4 = \frac{I_1 l}{2c_1}(c_1 - c),$$

$$\gamma_5 = \frac{I_2 l}{2c_2}(c_2 - c), \quad \delta_1 = \frac{\sqrt{3}}{4} l, \quad \delta_2 = \frac{Il}{4c},$$

$$\delta_3 = \frac{I_1 l}{4c}, \quad \delta_4 = \frac{\sqrt{3}\, l}{c_1}, \quad \delta_5 = \frac{I_1 l}{2c_1},$$

$$\delta_6 = \frac{Il}{2c_2}, \quad c = n(n+1), \quad c_1 = n_1(n_1 + 1),$$

$$c_2 = n_2(n_2 + 1)$$

and

$$I = \int_{-1}^{1} P^l_{n_1}(\mu)\, P^l_{n_2}(\mu) \frac{\mathrm{d}\, P_n(\mu)}{\mathrm{d}\mu}\, \mathrm{d}\mu$$

$$I_1 = \int_{-1}^{1} [P^l_{n_1}(\mu)]^2 \frac{\mathrm{d}\, P_n(\mu)}{\mathrm{d}\mu}\, \mathrm{d}\mu$$

$$I_2 = \int_{-1}^{1} [P^l_{n_2}(\mu)]^2 \frac{\mathrm{d}\, P_n(\mu)}{\mathrm{d}\mu}\, \mathrm{d}\mu$$

If the components are chosen in such a way that cross-equatorial flow is avoided and the flow is thus confined to one hemisphere only, all the constants appearing in eq. (7) are non-zero. Even though tropical influences may be important for the blocking phenomenon in midlatitudes (see Webster, 1981), the simplifying assumptions involved in this model (i.e. quasi-geostrophy) do not allow a realistic description of cross-equatorial flow.

The steady-state properties of (7) for varying values of the orographic and the vorticity forcing may be found by solving (7) for the stream function amplitudes with all the time derivatives set to zero. Because of the non-linearities in (7) it is possible to have multiple steady-state solutions for constant values of the forcing parameters. The bifurcation properties of the low-order system may be investigated by plotting one of the steady-state amplitudes as a function of one of the forcing parameters (while all of the other forcing parameters are held constant).

It may first be noted that the equations for $\dot{x}_1 = 0$, $\dot{y}_1 = 0$, $\dot{x}_2 = 0$ and $\dot{y}_2 = 0$ are linear in the amplitudes of the wave components. This means that the low-order system does not allow wave-wave to wave interactions. Solving for the wave amplitudes at a steady-state and inserting these solutions into the equations for $\dot{u}_0 = 0$ and $\dot{z} = 0$ we arrive at two non-linear equations in $u_0$ and $z$. Solving one of these, say $\dot{z} = 0$, for $u_0$ or $z$ involves the solution of a quartic equation. Regarding $z$ as a parameter in $\dot{z} = 0$ and solving for all the possible real values of $u_0$ we can finally arrive at one equation in one of the unknown steady state amplitudes, namely $\dot{u}_0(z) = 0$. This procedure can be done numerically and the results are most conveniently displayed in a diagrammatic form where the zonal forcing ($u_{0E}$) is plotted as a function of the steady-state amplitude, $z$.

An example of such a plot is given in Fig. 1. The forcing is chosen to represent conditions present in

the Northern Hemisphere during winter time. The orographic forcing is fixed at a value of 0.05 while the wave vorticity forcing has a varying amplitude, but the phase in relation to the orography is fixed. The zonal vorticity (or momentum) forcing is plotted on the vertical axis. Multiple steady states of the system are identified in the figure by the condition that a horizontal line should have multiple intersections with one of the steady state curves. The forcing parameters are in a range where multiple steady states are just possible, i.e. close to the first bifurcation point. For smaller values of the forcing parameters the non-linear system behaves quasi-linearly, with just one steady state for a certain value of the forcing parameters. By linearizing eq. (7) and computing the eigenvalues of the matrix governing the linearized motion around each of the steady states, stability properties are found as indicated in Fig. 1. It may be noted that no Hopf-bifurcations (see Marsden and McCracken, 1976) indicating the existence of limit cycles around the steady states have been found in this low-order model for reasonable values of the forcing parameters.

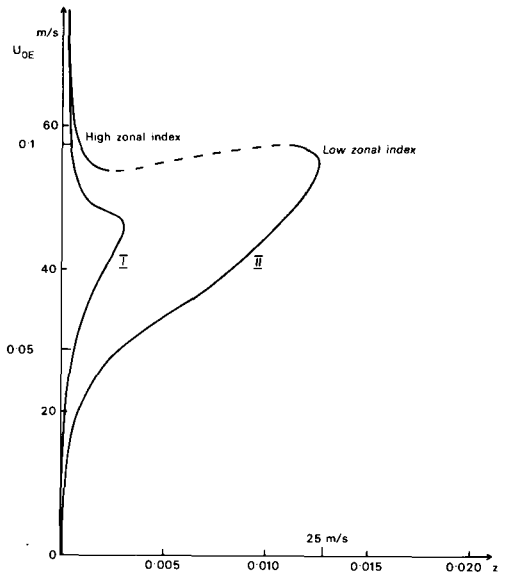


*Fig. 1.* Steady-state curves for the low-order model. The abscissa gives the response in terms of the amplitude of one of the zonal components ($z$), the ordinate gives the strength of the zonal forcing ($u_{0E}$). The dimensional units are taken as the zonal average at 45° latitude. For curve I there is no wave vorticity forcing while for curve II there is a wave vorticity forcing in the same component as the orography. The amplitude of the wave forcing is 20 $ms^{-1}$ in dimensional units and the phase angle is −90°. Stability properties as indicated by dashed (unstable) and full (stable) lines. Parameter values: $l = 3$, $n_1 = 4, h_1 = 0.05, \varepsilon = 0.06, x_{1E} = 0, y_{1E} = -0.015$.

K81 showed that the most favourable phase angle for multiple equilibria to exist is around −90°. This phase angle implies positive (cyclonic) vorticity forcing on the leeward side of the highs in the orography. For the curve marked I in Fig. 1 the wave vorticity forcing is set to zero and the only forcing of the model is in the orography and the zonal momentum. For the orography height chosen in Fig. 1 there is only one stable steady state for all values of the zonal momentum forcing. For higher values of the orographic parameter multiple, steady states are possible within certain ranges of values of the zonal momentum forcing. For further details of this, see K81.

Another way of obtaining a region of multiple equilibria is to include vorticity forcing in one of the wave components, and this is shown with steady-state curve II in Fig. 1. The phase of the wave vorticity forcing is −90°, i.e. the most favourable one for bifurcations to occur. K81 investigated the characteristics of the steady states within the region of multiple equilibria. It was found that the steady states on the left-hand, upper branch of curve II in Fig. 1 had a marked zonal flow and a rather weak wave component. The steady states on the right-hand branch, on the other hand, had a much stronger wave component and a weaker zonal flow. These latter steady states can be associated with low index atmospheric circulations, i.e. blocking periods, while the steady states on the left-hand branch have the characteristics of a high index, zonal type of circulation.

Examining the energetics of these two solution types it was found that in the zonal steady state the orographic influence on the flow was much weaker than in the blocked state. In the blocked state the orography acted to transform zonal kinetic energy into wave kinetic energy in a much more intense way than in the zonal state. Furthermore, the efficiency of the flow in picking up energy from the wave vorticity forcing was markedly different. In the blocked flow the phase difference between the forced wave and the wave forcing is very small, thus giving a high amplitude response. In the zonal steady state, the trough on the leeward side of the orography is further downstream from the orographic high than in the blocked case, and the

response amplitude is thus lower. The unstable steady states on the dashed part of curve II have properties somewhere intermediate between the two stable branch steady states. The unstable steady states are, of course, not very interesting. Because of their instability the flow will never settle into them.

Even if the stream patterns obtained with the extremely simplified low-order model bear no close resemblance to real atmospheric flow, it is hoped that the mechanisms leading to the bifurcation into multiple equilibria have their counterparts in the real atmosphere. From the energetics calculated in K81 one may conclude that in the "blocked" stable equilibrium the waves generated by the orography and the wave vorticity forcing reinforce each other to give a pronounced wave component of the flow. Energy is thus taken from the zonal flow and transferred to the waves via the effect of the orography. In the zonal steady-state the orographic lee wave is not as pronounced and the amount of energy transferred from the zonal flow to the eddies is not as large as in the blocked steady state. The effect of the orography on the flow pattern is thus smaller in the zonal steady state than in the blocked one. The orography can also be seen to act as a triggering mechanism, directing the basically vorticity forced flow into one or other of the stable equilibria.

## 3. High-resolution experiments

A serious shortcoming of a severely truncated low-order system is the lack of interaction between waves of all scales. Only a few scales of motion are taken into account and the interactions with other scales are either neglected completely or included via a bulk momentum forcing. To investigate whether the bifurcation mechanism found in the low-order model of Section 2 is sensitive to the number of waves present in the model, experiments have been performed with a high-resolution quasi-gestrophic, spectral, barotropic model. This model was originally developed at the University of Reading, England, and it is a barotropic and quasi-geostrophically balanced version of the model described by Hoskins and Simmons (1975). The governing equation of the model is the same as in Section 2, i.e. eq. (1). Forcing is introduced in exactly the same components as in the low-order model and the model is integrated in time to find the steady state(s). For reasons of economy, most of the experiments were done with a T21 truncation ($m \leq 21$ and $n \leq 21$ in the Legendre representation). However, some integrations done with a T42 truncation showed no significant differences to the T21 experiments.

To find multiple stable steady states, the time integrations are set up in the following manner. Initially the forcing is held constant for a time period of 20 days. The model, starting from a state of rest, is allowed this time to find a steady state. As can be seen from Fig. 2, this time period is sufficient for the initial oscillations to damp down. This is mainly due to the high dissipation rate (see below). After the model has settled into a steady state, the zonal momentum forcing is slowly increased or decreased in time. The time scale of this slow increase or decrease is chosen to be significantly slower than the dissipation time scale of the model (the forcing is doubled or halved in 100 days while the dissipation time scale is around 2.5 days). In this way it is hoped that the model stays reasonably close to a stable state all of the time. If, however, a bifurcation of the type pictured in Fig. 1 occurs, the model has to make a sudden jump from one stable branch of the steady-state curve to the other when a critical value in the zonal forcing is passed. In a time plot of some of the spectral coefficients, this will show up as a sudden change of the amplitude and perhaps some damped oscillations when the model settles into a steady state on the other branch.

Results of experiments of this kind are displayed in Fig. 2. The forcing parameters have values which are close to the ones used in the low-order example of Fig. 1. The phase difference between the wave vorticity forcing and the orography is exactly the same, $-90°$. It was found, however, that in order to obtain multiple equilibrium states with a high-resolution model, the vorticity forcing has to be higher. This is presumably due to the fact that the existence of more components forces the energy introduced at certain wave components to spread out to all parts of the spectrum. The long waves therefore need more energy input to reach the critical amplitudes necessary for bifurcations to occur. The orography, on the other hand, had to be lowered to avoid the formation of multiple equilibria when only zonal momentum forcing is present. The high-resolution model thus appears to be more sensitive to the height of the orography than the low-order model.

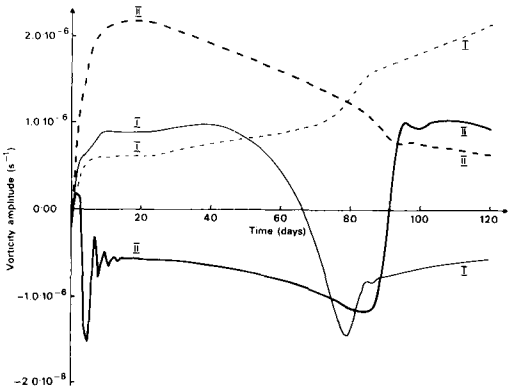


*Fig. 2.* Vorticity amplitudes of one wave component ($k = 3$, $n = 4$; solid curves) and one zonal component ($k = 0$, $n = 1$; dashed curves) as a function of time in the high-resolution model. Curves marked I refer to the experiment with increasing zonal forcing, the ones marked II to a decreasing zonal forcing. ($\varepsilon = 0.06$, $h = 0.025$, $x_{1E} = 0$, $y_{1E} = -0.02$, $u_{0E} = \{^{0.05+}_{0.15-}\}$ (time-20)*0.001, time in days.)

In Fig. 2 the amplitudes of the forced zonal and wave components are shown as a function of time for two different experiments. In one experiment (curves marked I) the zonal forcing starts at a fairly low value, well below the bifurcation "knee" of the curve in Fig. 1. After day 20 the zonal forcing is increased slowly and from the amplitudes of the forced zonal component and the forced wave component it can be seen that a sudden jump occurs around day 80. The curves marked II show a similar experiment, but this time the zonal forcing is decreasing as a function of time. In these curves the jump occurs around day 90 and it should be noted that the jump does not occur at the same value of the zonal forcing as for the jump with an increasing zonal forcing. This strongly suggests that there is a certain interval in the values of the zonal forcing where multiple stable steady states are possible. To find these steady states, the same type of integrations have been performed, but instead of increasing/decreasing the zonal forcing until the end of the integration, the zonal forcing was held constant at a certain level after an increase/decrease from an initially low/high value. The final level of the forcing was chosen to be in the range of possible multiple equilibria. In Plate 1 the stream-functions found in such an experiment are displayed. The top figure is the steady-state which is reached from an initially high value of the zonal forcing; the lower part is the steady-state reached from an initially low value of the zonal forcing. Comparing these figures with the low-order results of K81 it may be concluded that the stream patterns are qualitatively similar. One has a pronounced wave component and can be interpreted as a blocked steady state. The other has a much more marked zonal flow and a weaker wave component. The feature displayed in Fig. 1 (and where it is shown in K81 that when orography alone is not sufficient to produce a forcing regime with multiple equilibria, a combination of orographic and wave vorticity forcing does give this possibility) is reproduced by the high-resolution model. The addition of wave vorticity forcing is thus not just a linear addition of wave energy to the flow; instead it actively takes part in the non-linear formation of multiple equilibria.

Examination of the steady states for other values of the zonal forcing have shown that all steady states on the left-hand, stable branch of the bifurcation curve in Fig. 1 have characteristics similar to the top flow of Plate 1, while the steady states on the right-hand part of the bifurcation curve have characteristics similar to the lower part of Plate 1. The steady-state branch which resembles a "blocked" flow is closely associated with a resonance of the forced Rossby wave. One of the steady-state branches can thus be seen as a resonant branch while the other is far removed from resonance. For sufficiently high values of the orographic and the wave vorticity forcing it is possible to have a situation where these branches are partly overlapping, and where multiple equilibria are possible for a certain constant forcing.

The numerical experiments with the high-resolution spectral model thus strongly support the results derived from the low-order model in Section 2 and K81. There are, however some aspects of the low-order model behaviour which are not verified by the high-resolution experiments. One such behaviour is the bifurcation obtained in a low-order model in the absence of orography. With a low-order model it is possible to find multiple equilibria with only stream function forcing on the longer waves. In the low-order study of Vickroy and Dutton (1979), three components were involved and their results indicated that a non-linear instability, due to the interaction beween one zonal component and two different wave components, may arise in quasi-geostrophic, barotropic flows. Wiin-Nielsen (1979) studied the non-linear proper-

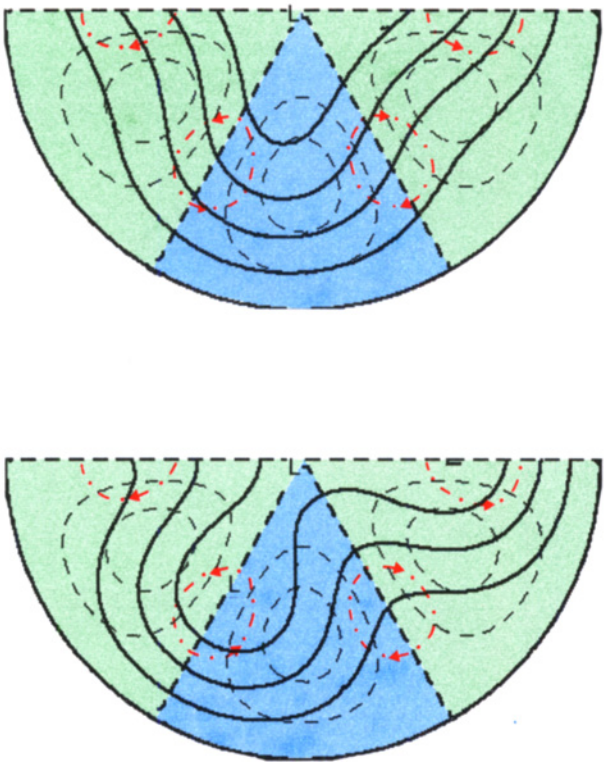

*Plate 1* Two stable stream-function patterns ($\varepsilon$=0.06, h=0.025, $x_{1E}$=0.0, $y_{1E}$=0.02, $u_{0E}$=0.095). Full lines are isolines for the stream-function with the same isoline interval in the two plots. Dashed lines are isolines for the orography, areas with the orography above its mean value (land areas) are green while areas with the orography below its mean value (ocean areas) are blue. The red dashed-dotted curves indicate the positions and directions of maximum and minimum wave vorticity forcing.

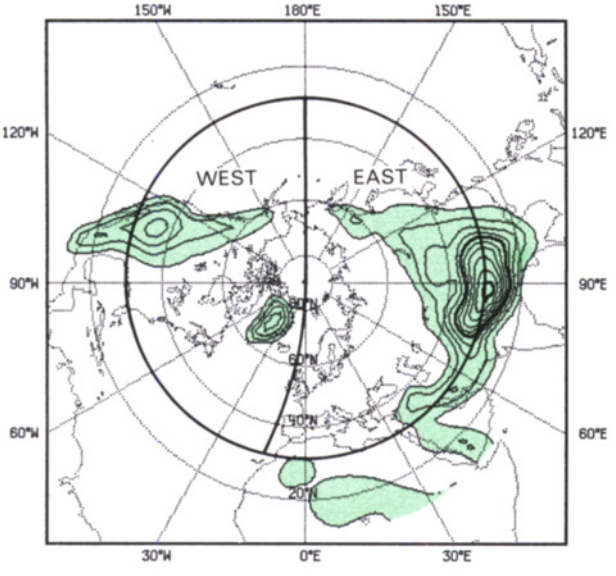


*Plate 2* Geographical map of the orographic field used to calculate the mountain torque. Contours are drawn with a 500 m interval. Areas with mountains higher than 500 m are green. Thick lines indicate the boundaries of the western and eastern regions used for the calculation of the separate contributions to the mountain torque.

TIME AVERAGED 500 mb SURFACE

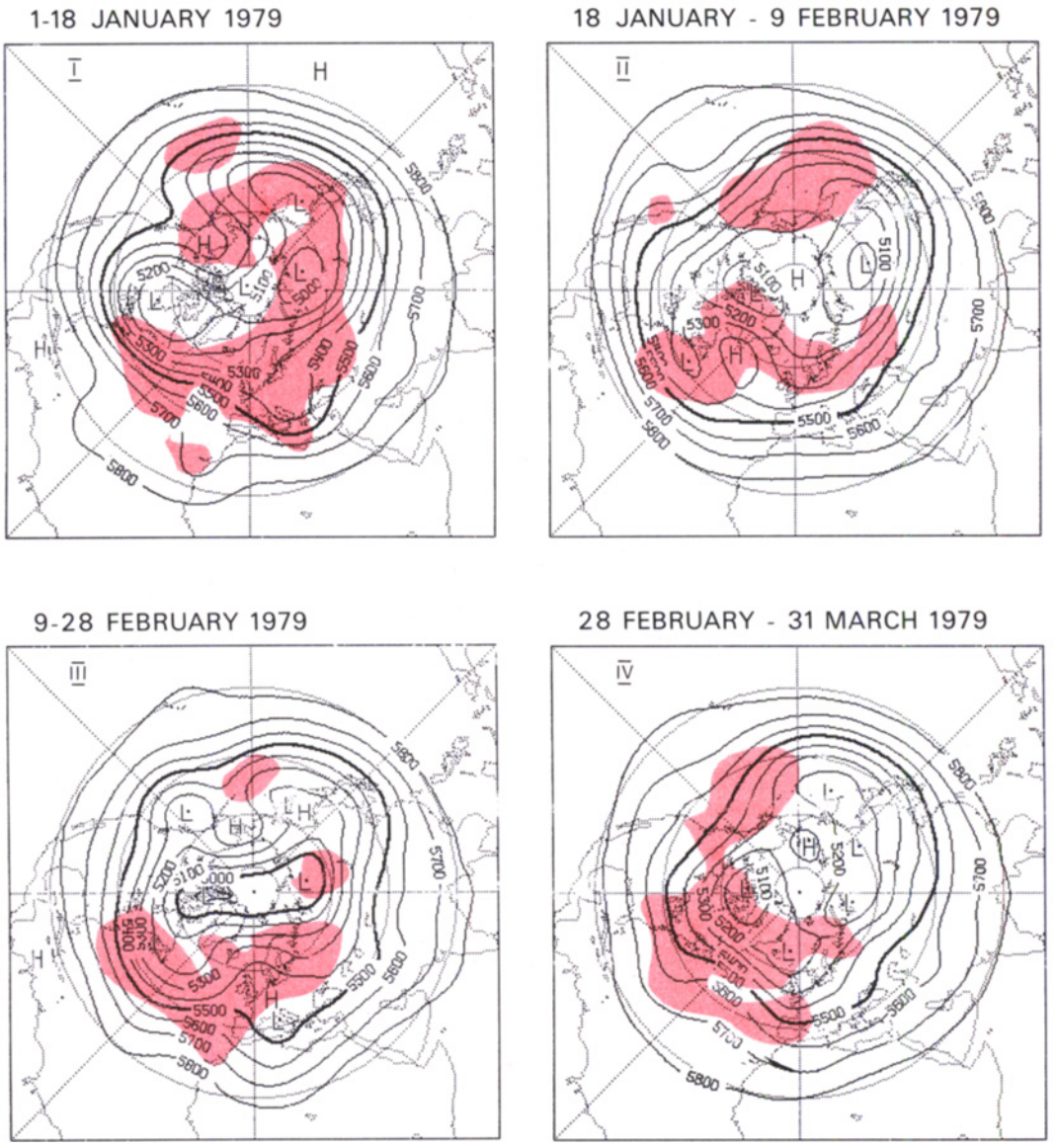


*Plate 3* Time mean maps of the 500 mb surface for the time periods indicated in Fig. 3. Areas where the square root of the variance is above 120 m are red.

ties of a five-component model on the sphere with a Newtonian type of forcing. With forcing on a component which describes cross-equatorial flow, he obtained a bifurcation and found two stable equilibrium states for a fixed value of the forcing parameter. The model studied in Wiin-Nielsen (1979) is very similar to the low-order model described in Section 2, and it can be shown that a bifurcation is possible in the low-order model of this study even in the absence of orographic forcing. Neither the results from Wiin-Nielsen (1979) nor Vickroy and Dutton (1979) were verified with a high-resolution model, and experiments with the high-resolution model of this study have not shown this feature, even for very large values of the forcing parameters. This may partly be due to the fact that in Wiin-Nielsen (1979), the forcing is introduced in a component which involves cross-equatorial flow. This model, however, behaves perfectly linearly when only momentum forcing is applied, the response to the forcing being purely in the forced components. For shorter waves this is no longer true. Hoskins (1973) has demonstrated that for zonal wave numbers larger than 5 a non-linear instability develops which is mainly due to wave-wave interactions. For the longer waves, the Coriolis effect acts as a stabilizing factor which prevents this type of non-linear instability. With orography present, it thus seems that a new type of instability develops as first pointed out by Charney and DeVore (1979).

An intuitive reasoning which points to a possible reason for this property of the orography can be given as follows. The governing equation of the model (1) at a steady state may be written

$$J(\zeta, \psi) + J(h, \psi) - \frac{2\partial\psi}{\partial\lambda} + \varepsilon(\zeta_E - \zeta) = 0 \qquad (8)$$

If $h = 0$ (no orographic forcing) and $\zeta_E \neq 0$, it is possible to have a steady state where the response is in the same component as the forcing and the non-linear term $J(\zeta, \psi)$ is zero. As mentioned above, numerical experiments with reasonable values of the vorticity forcing on the longer waves have shown that such a steady state is stable. Equation (8) is in this case linear. This also holds if the wave vorticity forcing is applied at several low wave numbers simultaneously. If an orographic forcing is introduced ($h \neq 0$) the term $J(h, \psi)$ forces energy introduced via the vorticity forcing $\zeta_E$ at a certain wave number to spread over the whole spectrum. It is this energy spread combined with a suitable vorticity forcing that appears to give rise to a non-linear instability and the bifurcation leading to multiple steady states. The experiments with the high-resolution model have also confirmed that a suitably positioned vorticity forcing in a wave component enhances this bifurcation mechanism.

## 4. Observational study of some blocking events

The main conclusion that can be drawn from the bifurcation mechanism investigated in a barotropic model is that the orography is necessary as a triggering mechanism in establishing the multiple steady states. The implied application of the theory to atmospheric blocking can thus be tested by studying the effect of the orography on the atmospheric flow in connection with blocked flow situations. One parameter which reflects the influence of the orography on the barotropic component of atmospheric flow is the mountain torque. In addition, to couple observational evidence with the proposed combination of orographic and wave vorticity forcing, an evaluation of the long-wave forcing is needed. This forcing should be seen as the cumulative effect of the transient eddies on the mean flow rather than a direct thermal forcing. The eddies generated by baroclinic instability processes have a much shorter scale than the long waves which are responsible for the bifurcation mechanism discussed in this study. A number of diagnostic studies, however, have, shown that the non-linear energy transfer from the baroclinic eddies to the long waves is a characteristic feature of atmospheric flow (see for example Saltzman, 1970 and Steinberg et al., 1971).

To study the orographic factors influencing blocking action in the Atlantic and Pacific regions separately, it is necessary to separate the torque contributions from the American and the Eurasian continents. It is primarily downstream from a mountain range that the orography may influence the flow pattern. The mountain torque parameter essentially reflects the surface pressure distribution around a mountain range and therefore it would be possible to separate the contributions from each continent by computing the torque for the eastern and western parts of the Northern Hemisphere separately. The separation line between eastern and

western parts would then have to lie entirely within the oceanic regions.

The zonal angular momentum balance at a given point in the atmosphere may be written

$$\frac{\partial M}{\partial t} = -\nabla_3(M\mathbf{v}_3) - g\frac{\partial Z}{\partial \lambda} + F_\lambda a\cos\varphi \qquad (9)$$

where $M$ is the angular momentum $(u + a\Omega\cos\varphi)\, a\cos\varphi$, $\mathbf{v}_3$ the three-dimensional velocity vector, $Z$ the height of a constant pressure surface, and $F_\lambda$ the frictional forces in the zonal direction. Integrating this equation vertically and over an area ($A$) which encircles one complete land mass (boundaries in oceanic areas), we obtain

$$\int_A\int_0^{p_s}\frac{\partial M}{\partial t}\frac{a\cos\varphi}{g}\,\mathrm{d}p\mathrm{d}S =$$

$$-\int_A\int_0^{p_s}(\nabla_3 M\,\mathbf{v}_3 - F_\lambda a\cos\varphi)\frac{a\cos\varphi}{g}\,\mathrm{d}p\mathrm{d}S$$

$$-\int_A p_s\frac{\partial h}{\partial\lambda}a\cos\varphi\,\mathrm{d}S \qquad (10)$$

where the mountain torque, $T_M$, within the area is given by the term

$$T_M = -\int_A p_s\frac{\partial h}{\partial\lambda}a\cos\varphi\,\mathrm{d}S \qquad (11)$$

The $p_s$ is here the surface pressure, and using standard atmospheric data given on pressure levels and at sea level, an interpolation has to be made to find $p_s$. The vertical interpolation is done here with cubic splines, but using other interpolation methods did not appear to change the results significantly.

A time period during which many blocks occurred in the Northern Hemisphere and for which a high quality set of atmospheric data is available is January–March, 1979. This time period falls within the FGGE year and the data used for all the calculations presented here is the FGGE level IIIb data (see Bengtsson et al., 1981).

Calculations of the quantity $T_M$ defined in eq. (11) were made over the areas defined in Plate 2, and a time plot of the torque for the two areas is shown in Fig. 3. The time evolution of the mountain torque has been smoothed with a 5-day running time mean to remove the influence of short-lived, travelling baroclinic eddies. These tend to give large variations in the torque on a time scale of 1 day. The mean value of the torque is very much influenced by the choice of the southern boundary for the calculations while the shape of the mountain torque curve is not very sensitive to the position of the southern boundary.

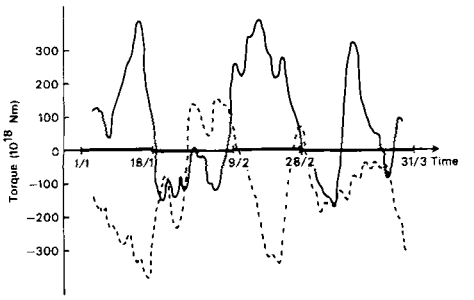


*Fig. 3.* Mountain torque for western (full line) and eastern (dashed line) parts of Northern Hemisphere (30° N–90° N) during January–March, 1979. The curves are calculated from 12-hourly FGGE data, and a running 5-day mean time filter has been applied to smooth the curves. The time periods which are used as averaging periods for Plate 3 are indicated on the horizontal time axis.

The most prominent feature of the curves in Fig. 3 is the large variation of the torque on a time scale of about 2 weeks. Both curves tend to show sudden jumps between what appears to be fairly constant values, the jumps appearing over a time interval which is shorter than the time scale over which the torque is approximately constant. To investigate whether there is any relation between the periods of low values of the torque (negative values of the torque imply a mountain drag) and the blocking events during January–March 1979, time mean maps of the 500 mb flow have been prepared for the time periods indicated in Fig. 3. The time periods are chosen to coincide with the periods between the jumps in Fig. 3. For the four time periods the mean flows are displayed in Plate 3. Also shown in Plate 3 are areas with a high value of the time variability of the 500 mb surface height. The variability is calculated as the standard deviation of the 12-hourly values from the period average. A high variability indicates an intense eddy activity which can be coupled to strong baroclinic developments at midlatitudes. A time plot of the variability averaged over regions upstream of the characteristic blocking regions is shown in Fig. 4. The variability in this figure is calculated as the standard deviation from a running 7-day average of the 500 mb surface height. A high

value of this quantity may thus be interpreted as an intense activity of eddies with a characteristic life time which is between 12 h and 7 days.

The time series has been divided into the following four periods:

I 1 Jan 1979–18 Jan 1979
II 18 Jan 1979–9 Feb 1979
III 9 Feb 1979–28 Feb 1979
IV 28 Feb 1979–31 Mar 1979

During periods I and III there are well-developed ridges over the Pacific Ocean and the ridge in period III has many of the characteristics of a blocked flow. In the Atlantic region there is a well-developed block during period II while there is a tendency for some ridging over Europe during period III. During period IV there is a predominantly zonal flow over the Atlantic–European region while over the Pacific there is a strong ridge in the poleward part of the region, while the flow is zonal across the central Pacific Ocean. Going back to the plot of the mountain torque (Fig. 3), one may see that the Atlantic block during period II and the Pacific block during period III are coupled with low, negative values of the torque, i.e. a mountain drag. The Pacific ridge during period I is also associated with a high mountain drag over the Eurasian continent while the zonal flows over the Atlantic region during periods I and III and over the Pacific during period II are coupled with high, positive values of the torque. During the last period (IV) the torque from the North American continent shows considerable fluctuations and the flow over the Atlantic and European regions is predominantly zonal. The torque from the Eurasian continent is distinctly negative and there is a ridge extending northwards towards the polar regions over the Pacific Ocean. The occurrence of a high mountain drag thus has some correspondence with the appearance of a blocking high downstream of a continent.

The influence of the transient motion on the time mean flow is the mechanism which in the barotropic model is represented by a direct vorticity forcing. Evaluating this vorticity forcing from atmospheric data is difficult as discussed by Savijärvi (1978). Some attempts have been made at calculating the vorticity forcing for the time periods indicated in Fig. 3, but the results have generally been noisy and it has been difficult to see any clear pattern. Instead, the eddy activity has been evaluated in terms of the standard deviation of the 500 mb surface during the different time periods. From Plate 3 it may be seen that the eddy activity upstream of a blocking region has some connection with the time periods defined earlier. Through Fig. 4 it may be seen that the Atlantic blocking during period II and to some extent the Pacific blocking during period III are coupled with a strong eddy activity in the beginning of those periods. However, as the blocking period continues there seems to be a decline in the activity of the eddies, especially during period II and in the Atlantic region. The decay of the block may therefore be coupled with the declining eddy activity; when the block has disappeared there is a renewed intensification of the eddy activity. This reasoning does not hold with the period III block in the Pacific region, there the blocking is preceded by a very low eddy activity. On the geographical maps (Plate 3) it may however be seen that there is a small region with a fairly high eddy activity just upstream of the block and it may be that the procedure of averaging the variance over a large area smooths this feature out. In any case, the geographical maps clearly show that the upstream flanks of the blocked regions do have intense eddy activity on the average and this is to be expected from the well-known fact that in the Gulf Stream and Kuroshio regions of the Atlantic and Pacific Oceans respectively, there is normally an intense baroclinic activity.

The ridge over Europe during period III, which on the daily 500 mb maps can be associated with

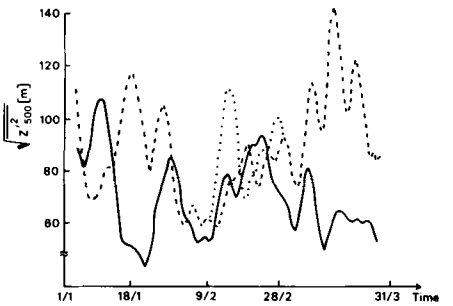


*Fig. 4.* Time evolution of variances as calculated from deviations of the 500 mb surface from a 7-day running mean and spatially averaged over certain regions. All regions extend from 30° N to the North Pole and have the following longitudinal boundaries: full line, 135° E–180° E (Kuroshio region of Pacific Ocean); dashed line, 45° W–90° W (Gulf Stream region of Atlantic Ocean); dotted line, 0°–45° E (European region).

blocking-like patterns, is not connected with a high mountain drag over the American continent. This may be explained by the fact that the ridge is too far downstream from the orography to be significantly influenced by it and the blocking ridges may therefore develop due to some other mechanism. From the plot of the variances of the 500 mb surface (Fig. 4) it may, however, be noted that within the European area there is quite a large variability during this time period. This can be due to blocking-like ridges moving across the area and not remaining stationary which also gives a smoothed ridge on a time averaged map. It may thus be a situation in which transient ridges develop but because of the orientation of the large-scale flow and the effect of the orography the ridges cannot remain stationary to form a persistent block.

## 5. Discussion and conclusions

In this paper it has been demonstrated that the results found by K81 for a low-order model on the sphere, are also found in a high-resolution, spectral model on the sphere with many more degrees of freedom. A combination of orographic, zonal momentum and wave vorticity forcing in a barotropic, quasi-geostrophic model on the sphere gives rise to a long-wave instability and the development of multiple, stable equilibrium states. One of these stable states can be associated with a large amplitude wave response, while another has a dominating zonal flow and a less pronounced wave component. The large-amplitude wave response (or blocked response) is close to a resonant flow configuration, where the wave response is almost in phase with the wave forcing. The zonal steady state is further removed from resonance and the response in the wave component is much smaller. Instead, due to the changed phase relationship between the wave and the orography, the zonal flow is more intense and the mountain drag is lower. These two types of equilibria can exist for the same values of all the forcing parameters; which one the flow chooses is crucially dependent on the initial state of the flow in relation to the unstable steady state.

The forcing parameters required in the barotropic model for the development of multiple equilibria, can be associated with the conditions present in the Northern Hemisphere during winter time. A strong zonal flow and an intense baroclinic eddy activity off the eastern coasts of the two major continents can thus be linked with two possible types of response of the long waves in the atmosphere. Once the atmosphere has settled into one of these response types it is likely to remain there for an extended period of time due to the stability of the flow configuration. In one of the response types there is a well-developed ridge downstream of a continent and this ridge can be associated with a blocked flow. A blocking ridge should be accompanied by a high mountain drag upstream of the block, a feature which has been found in Section 4 for some blocking situations. To remain in this near resonant flow configuration, it is also necessary that the eddy activity upstream of the blocking ridge is maintained to give an input of kinetic energy on the longer waves. From the diagnostic studies of Section 4 it appears that this eddy activity steadily decreases during a blocking event and this may be the cause of the vanishing of the blocking ridge. A decreased eddy activity would, according to the barotropic mechanism put forward in Section 3, imply that the blocked steady state vanishes (for a constant zonal forcing), the flow being forced to settle into a zonal flow configuration. In Fig. 1 this may be visualized as the disappearance of curve II when the flow has settled into a state on the low index branch of curve II. At a critical value of the eddy forcing on the long waves, the flow would be forced to transfer to a more zonal type of circulation.

The diagnostic studies in Section 4 of 3 particular winter months indicate that a mechanism involving the effect of the orography and the effect of the eddies on the time mean flow has some connection with the occurrence of blocked flows. The bifurcation mechanism proposed in this study does not disagree with the results obtained from the limited diagnostic study of Section 4. However, it should be stressed that the diagnostic study does not confirm that a bifurcation mechanism is active in the formation of a blocked flow, and because of the limited time period the results may not be statistically significant. A more complete diagnostic study of the mountain torque and the eddy activity during several winters with many blocking events is needed to say anything conclusive about the cause of blocking events.

The results showing the connection between the

drag of a mountain ridge on the scale of a continent and the occurrence of a blocked flow downstream of that continent are, however, very suggestive. The orographic drag is likely to help to create a large-amplitude wave downstream of the orographic barrier. In the bottom flow diagram of Plate 1, the "blocked" steady-state ridge does, however, not resemble a blocking high in the atmosphere. The omega shaped contours are missing and the so-often observed dipole structure with a low south of the blocking high is also missing. Some other mechanism(s) must thus also be involved to explain all aspects of the formation of blocking ridges. It may be that the "blocked" steady state of the bifurcation theory gives a region inside which a blocking ridge may easily form, but the more detailed structures of a blocking high could perhaps be explained by a theory based on soliton solutions of the barotropic vorticity equation as proposed by McWilliams (1980).

To investigate more closely how the eddies affect the time mean flow and, equally important for the breakdown of the block, vice versa, a model involving baroclinicity must be used. The baroclinic processes are not necessarily important on the same scale of motion as the orographic long-wave instability, but should rather be incorporated on a much shorter scale where the baroclinic instability process is active. These two scales of motion may then be coupled through purely barotropic processes transporting energy between different parts of the spectrum via wave-wave interactions. With such a model it may be possible to investigate more closely the findings in Section 4 that the eddy activity upstream of a blocking region decreases during the course of a blocking event. This kind of model could thus give more insight into the atmospheric processes which in the barotropic model are simulated by a direct vorticity forcing on the long waves.

## 6. Acknowledgements

The author would like to thank A. Simmons for help and advice in running the high-resolution spectral model and M. Kanamitsu for help in connection with the use of FGGE data. Additionally, the author is very grateful for the technical assistance provided by Mrs R. Shambrook and the ECMWF print room in producing the colour plates.

## REFERENCES

Bengtsson, L., Kanamitsu, M., Kållberg, P. and Uppala, S. 1981. The FGGE III-b system at ECMWF. To appear in *Bull. Amer. Meteorol. Soc.*

Charney, J. G. and DeVore, J. G. 1979. Multiple flow equilibria in the atmosphere and blocking. *J. Atmos. Sci. 36*, 1205–1216.

Davey, M. K. 1980. A quasi-linear theory for rotating flow over topography. Part I: Steady $\beta$-plane channel. *J. Fluid Mech. 99*, 267–292.

Davey, M. K. 1981. A quasi-linear theory for rotating flow over topography. Part II: Beta-plane annulus. *J. Fluid Mech. 103*, 297–320.

Hoskins, B. J. 1973. Stability of the Rossby-Haurwits wave. *Q. J. R. Meteorol. Soc. 99*, 723–745.

Hoskins, B. J. and Simmons, A. J. 1975. A multi-layer spectral model and the semi-implicit method. *Q. J. R. Meteorol. Soc. 101*, 637–655.

Källén, E. 1981. The non-linear effects of orographic and momentum forcing in a low-order, barotropic model. *J. Atmos. Sci. 39*, 2150–2163.

Marsden, J. E. and McCracken, M. 1976. *The Hopf bifurcation and its applications.* New York: Springer Verlag, pp. 408.

McWilliams, J. C. 1980. An application of equivalent modons to atmospheric blocking. *Dyn. Atmos. Oceans 5*, 43–66.

Saltzman, B. 1970. Large-scale atmospheric energetics in wave number domain. *Rev. Geophys. and Space Phys. 8*, 289–302.

Savijärvi, H. 1978. The interaction of the monthly mean flow and large scale transient eddies in two different circulation types, Part II. *Geophysica 14*, 207–229.

Steinberg, H. L., Wiin-Nielsen, A. and Yang, C.-H. 1971. On non-linear cascades in large-scale atmospheric flow *J. Geophys. Res. 76*, 8629–8640.

Vickroy, J. G. and Dutton, J. A. 1979. Bifurcation and catastrophe in a simple, forced, dissipative quasi-geostrophic flow. *J. Atmos. Sci. 36*, 42–52.

Webster, P. J. 1981. Mechanisms determining the atmospheric response to sea surface temperature anomalies. *J. Atmos. Sci. 38*, 554–571.

Wiin-Nielsen, A. C. 1979. Steady states and stability properties of a low-order barotropic system with forcing and dissipation. *Tellus 31*, 375–386.